Structural features of the glutamate-binding protein from *Corynebacterium glutamicum*

Alessandro Capo[1], Antonino Natalello[2], Jan Marienhagen[3,4], Angela Pennacchio[1], Alessandra Camarca [1], Stefano Di Giovanni[1], Maria Staiano[1], Sabato D'Auria[1*], Antonio Varriale[1]

[1]Institute of Food Science CNR, via Roma 64, 83100 Avellino, Italy
[2]Department of Biotechnology and Biosciences University of Milano-Bicocca P.zza della Scienza 2, 20126 Milano, Italy
[3]Institute of Bio- and Geosciences, IBG-1: Biotechnology, Forschungszentrum Jülich, 52425 Jülich, Germany
[4]Institute of Biotechnology, RWTH Aachen University, Worringer Weg 3, D-52074 Aachen, Germany

*Correspondence to:

Dr. Sabato D′Auria
Institute of Food Science, CNR
Via Roma, 64, 83100 Avellino
Italy
Phone: +39-0825299101
Fax: +39-0825299100
Email: sabato.dauria@cnr.it

Abstract

L-glutamate (Glu) is the major excitatory transmitter in mammalian brain. Inadequate concentration of Glu in the brain correlates to mood disorder. In industry, Glu is used as a flavour enhancer in food and in foodstuff processing. A high concentration of Glu has several effects on human health such as hypersensitive effects, headache and stomach pain. The presence of Glu in food can be detected by different analytical methods based on chromatography, or capillary electrophoresis or amperometric techniques. We have isolated and characterized a glutamate-binding protein (GluB) from the Gram-positive bacteria *Corynebacterium glutamicum.* Together with GluC protein, GluD protein and the cytoplasmic protein GluA, GluB permits the transport of Glu in/out of cell. In this study, we have investigated the binding features of GluB as well as the effect of temperature on its structure both in the absence and in the presence of Glu. The results have showed that GluB has a high affinity and selectivity versus Glu (nanomolar range) and the presence of the ligand induces a higher thermal stability of the protein structure.

Keywords

Glutamate binding protein, Corynebacterium glutamicum, Fluorescence spectroscopy, FT-IR

1 Introduction

Glu is the major excitatory neurotransmitter of the human brain [1]. Different studies have demonstrated a correlation between anomalies in Glu signalling and different neuro-generative psychiatric disorders such as schizophrenia [2], alcohol dependence [3], and obsessive-compulsive disorder [4] and, more in general, with mood-related disorders. These studies have demonstrated that the increase of plasma Glu level is associated with mood disorders. On the contrary, Glu is extensively used in the food industry as a flavor enhancer of various foodstuffs. High concentrations of Glu could have hypersensitizing effects on human health such as headache, stomach pain [5]. High Glu level has been also linked to Chinese Restaurant Syndrome (CRS) [5]. CRS refers to a group of symptoms that some people experience after eating food from a Chinese restaurant. It is known as monosodium glutamate MSG symptom complex, and often it includes headache, skin flushing, and sweating.

In biomedicine and food safety, different analytical methods have been developed for detection of Glu. These methods are based on amperometric [6], chromatography [7]and capillary electrophoresis [8] techniques. Due to the high operational complexity of these methods, there is an urgent need to monitor the presence of Glu in a more fast and easy way.

The development of advanced optical biosensors based on fluorescence and/or surface plasmon resonance techniques can overcome these drawbacks. The central core of these kind of biosensors is the molecular recognition element (MRE) that provides high specificity and sensibility to the device. In this context, we explored the possibility to use a specific substrate-binding protein (SBP) as molecular recognition element MRE for the detection of Glu. In all kingdoms of life, cells interact through an extremely elegant transport system, defined ATP-binding cassette (ABC) transporters. The function of this system is to uptake nutrients such as ions, cations and anions, amino acids, peptides, proteins, vitamins, drugs, fatty acids, and lipids into and out of cell. Different proteins constitute a typical ABC transporter: the protein soluble portion is named substrate-binding protein (SBP) in both the Gram-negative and Gram-positive bacteria. In particular, members

belonging this class of proteins are located in the periplasm of Gram-negative bacteria. Instead, they are lipid-anchored or fused to the two transmembrane domains (TMD) in Gram-positive bacteria and Archaea [9]. The common features of this class of protein family are low sequence similarity and high conserved structural fold, with two similarly folded domain connected with two-three stranded β-sheet [10]. SBPs are extensively used for biotechnological applications. Different studies showed the applicability of proteins belonging to this family as MREs in protein-based biosensor development [11-13]. In fact, different research groups are involved in the development of extremely sensitive biosensors, using SBPs for detection of small analytes with implication in food safety, environment and medical diagnostics. In the last two decades, our lab has contributed to enrich the knowledge in this field, with isolation and characterization of different substrate-binding proteins for application in fluorescence protein-based biosensors [11, 14].

With the aim to identify a possible candidate of MRE, we selected as SBP, a *putative* glutamate-binding protein (GluB) from the Gram-positive bacteria *Corynebacterium glutamicum*. This protein is involved in the uptake of Glu in this bacterium [15]. *Corynebacterium glutamicum* is a well-studied platform organism in industrial biotechnology [16, 17]. The most prominent application of this Gram-positive microorganism is the fermentative production of proteinogenic amino acids. Among them, L-glutamate and L-lysine that are used as flavour enhancer and the feed additive, respectively, are produced at a multimillion-ton-scale annually [18]. Furthermore, *C. glutamicum* strains have been engineered to produce numerous compounds of biotechnological interest such as organic acids [19], diamines and terpenes [20] and more recently diols [21] and polyphenols [22]. Recently GluB was crystallized, X-ray diffraction data set was collected and a structure model to a resolution of 1.9Å could be calculated [23].

In this study, we present the cloning, purification and a spectroscopic characterization of GluB. In particular, we explored the binding features and effect of temperature on the protein stability in the absence and in the presence of Glu in order to obtain information on GluB structural and functional

properties. The obtained data showed a high affinity of GluB versus Glu (nanomolar range) and the binding of Glu to GluB induced more stability to the protein structure.

2 Materials and Methods

2.1 Materials

Glu and DNase purchased from Sigma. Ampicillin, IPTG, lysozyme and all the reagents used in the preparation of LB medium and buffers were from AppliChem. All the other chemicals used were commercial samples of the purest quality. 2, 5-diphenyl-1, 3, 4-oxidiazole was purchased from Invitrogen.

2.2 Construction of pET22b (+)-gluB for the heterologous expression of gluB in E. coli

Recombinant DNA work, such as PCR, DNA restriction, or DNA ligation were carried out according to standard molecular cloning protocols [24]. If not stated otherwise, all enzymes were obtained from Thermo Scientific (Schwerte, Germany). The plasmid pET22b (+)-*gluB* was constructed for the heterologous expression of *gluB* from *C. glutamicum* in *Escherichia coli* BL21 (DE3). For this purpose, the *gluB* gene without the N-terminal signal sequence of 78 bps for the translocation into the periplasm was isolated by PCR using genomic DNA of *C. glutamicum* ATCC 13032 as a template. Necessary oligonucleotides (P*gluB*_C_his_*for*: 5′-AGCTGACATATGTGTGGTGATTCAAGCGGTGGCG-3′ (*Nde*I restriction site underlined) and P*gluB*_C_his_*rev*: 5′-GACAGTGCGGCCGCGCTTGCGTCGAGGAAGGAGAGGTCACC-3′ (*Not*I restriction site underlined) were ordered from Eurofins MWG Operon (Ebersberg, Germany) and the employed KOD Hot Start DNA polymerase was purchased from Merck (Darmstadt, Germany). The PCR program for the amplification of the desired *gluB* DNA sequence started with an initial denaturation step at 94°C for 2 min. Subsequently, 30 cycles (94°C, 30s; 60°C, 30s; and 72°C, 3s) and one fill-up cycle (72°C, 5 min) were performed. The resulting PCR product of approximately 850 bps in size was purified using the PCR purification kit (Macherey–Nagel, Dueren, Germany) according to manufacturer's instructions and quantified using a NanoDrop instrument (NanoDrop Technologies, Wilmington, DE, USA). Afterwards, the PCR-product was subjected to *Nde*I/*Not*I restriction and cloned into the equally digested pET22b (+) expression

vector. By design, gene expression from the resulting vector pET22b (+)-*gluB* attaches a C-terminal His_6-tag for the possibility of performing affinity purification of the truncated GluB protein. Finally, the agreement of the constructed plasmid with the *in silico* design was verified by DNA sequencing at Eurofins MWG Operon (Ebersberg, Germany).

2.3 Heterologous gluB-expression and protein purification

E. coli BL21 (DE3) was transformed with pET22b(+)-*gluB* and cultivated in LB medium in presence of 50µg/ml Ampicillin, until reaching an optical density at 595nm (OD_{595}) of 0.6, and GluB expression was induced with 0.8mM isopropyl β-D-1-thiogalactopyranoside (IPTG) overnight at 22°C. The cells were harvested by centrifugation at 4000 rpm at 4°C for 30 min, then they were suspended in Lysis buffer (20mM NaH_2PO_4/Na_2HPO_4, 500mM NaCl, 20mM imidazole, pH 7.4) with lysozyme (1mg/ml) and incubated for 30 minutes at 30°C. The suspension was sonicated (10 cycles, 30s on/30s off at 38% power), DNase (0.05mg/ml) and $MgCl_2$ (5mM) were added and incubated for 1h in ice. The lysate was centrifuged at 15000g at 4°C for 30 minutes. The obtained supernatant was filtered with a 0.22µm polyethersulfone (PES) syringe filter and purified using an AKTA FPLC system equipped with a HisTrap HP column (GE Healthcare). The flow-through was collected and the column washed with lysis buffer until the absorbance baseline was stable; then the protein was eluted at a flow rate of 5 ml/min with increasing concentration of imidazole (50-100-250mM imidazole). The purity of the eluted fractions was verified by gel electrophoresis (SDS-PAGE).

The fractions eluted at 50mM imidazole were concentrated with a centrifugal filter device (Vivaspin Turbo-Sartorius 30,000 MWCO) and were loaded onto a HiLoad 16/600 Superdex75 column equilibrated in PBS solution (6mM KH_2PO_4/Na_2HPO_4, 140mM NaCl, 3mM KCl, pH 7.4). The protein was eluted with PBS solution at a flow rate of 1ml/min, monitoring the absorbance of the eluate at 280nm. In order to verify the degree of purity of the obtained fractions, an SDS-PAGE (15%) was performed. The protein concentration was calculated on the absorbance values at 280nm

by using Lambert and Beer's law. The molar extinction coefficient, calculated using Expasy ProtParam, tool that follow the Edelhoch [25] method, is equal to 27515 M^{-1} cm^{-1}; the molecular weight is 32490 Da. Before to start experiments it was essential to remove the Glu bound to the protein following the purification. For this purpose, extensive dialysis of the isolated protein was performed against PBS pH 8.0 for five days.

2.4 Protein Analysis by MALDI-TOF MS

Identity of the truncated and C-terminal His-6-tagged GluB protein was confirmed by mass spectrometry. Therefore, proteins to be analysed by MS were excised in-gel trypsinized as described previously [26]. For protein identification by peptide mass fingerprinting, the tryptic peptides were subjected to MALDI-TOF MS using an Ultraflex III TOF/TOF mass spectrometer (Bruker Daltonics, Billerica, MA, USA). Mascot algorithm (Matrix Science, London, UK) was used to compare the experimentally determined peptide mass patterns with those of the entire *C. glutamicum* proteome.

2.5 Circular dichroism measurements

Circular dichroism (CD) measurements were performed on homogeneous samples of GluB (20 mM sodium phosphate, pH 7.4), with a protein amount of 0.15mg/mL in the absence or in the presence of the specified amounts of Glu.

We used the J-710 spectropolarimeter (Jasco, Tokyo, Japan) equipped with the Neslab RTE-110 temperature-controlled liquid system (Neslab Instruments, Portsmouth, NH). The instrument was calibrated with a standard solution of (+)-10-camphorsulfonic acid. Sealed cuvettes with a 0.1cm path length (Helma, Jamaica, NJ) were used. Photomultiplier voltage never exceeded 600V in the measured spectral region (190 to 250nm). Each spectrum was averaged five times and smoothed with spectropolarimeter system software, version 1.00 (Jasco, Japan). All measurements were

175 performed under nitrogen flow. Before undergoing CD analyses, all samples were kept at the
176 temperature being studied for 10 min. The results are expressed in terms of molar Ellipticity $[\theta]_{mrw}$.
177
178 *2.6 Steady-State fluorescence spectroscopy measurements*
179 Steady-state emission experiments were performed on ISS-K2 fluorometer (ISS, Urbana-
180 Champaign) equipped with a cell temperature-controlled sample holder. To selectively excite Trp
181 residues, the excitation wavelength was set at 295nm. Excitation and emission slit widths were
182 fixed at 0.5nm and 1.0nm respectively. Emission spectra recorded from 310nm and 410nm, at
183 1.0nm intervals. Samples were placed in the thermostatic holder and temperature of samples was
184 measured directly in the cuvette with an accuracy of ± 0.2°C. The buffer alone was used as blank
185 and its emission contribution was subtracted from the experimental spectra [27]. GluB binding
186 capability was studied by a fluorescence titration approach. For this purpose, recombinant GluB
187 (10µM) was titrated with increasing concentrations of Glu (0-100µM). In order to verify the GluB
188 binding specificity the binding of L-aspartate (Asp) was been investigated. The binding of amino
189 acids to GluB was estimated by a variation of the intrinsic protein fluorescence emission. The
190 maximal decrease of the protein fluorescence due to the saturation of the binding sites by the ligand
191 (F_{max}) was estimated from the titration data. Experimental data were processed by a non-linear
192 regression analysis computed with the OriginPro 8.0.
193
194 *2.7 Fluorescence Quenching*
195 Acrylamide quenching of the Trp fluorescence was observed at fluorescence maximum and
196 analysed by the Stern-Volmer equation:
197
198 $F_0/F = 1 + K_D[Q] = 1 + k_q\tau_0[Q]$ **Equation 1**
199

F_0 and F are the fluorescence intensities in the absence and presence of acrylamide, respectively; k_q is the bimolecular quenching constant; τ_0 is the lifetime of the fluorophore in the absence of quencher, and Q is the concentration of acrylamide. The Stern-Volmer quenching constant is given by $K_d = k_q\tau_0$. If the quenching is dynamic Kd will represent the Stern-Volmer constant. All fluorescence experiments were done in PBS buffer at pH 8.0 with the protein concentration of 0.05mg/mL. Quenching data are presented as plots of F_0/F versus $[Q]$. F_0/F is expected to be linearly dependent upon the concentration of quencher. A plot of F_0/F versus $[Q]$ yields an intercept of one on the *y*-axis and a slope equal to K_{sv}. A linear Stern-Volmer plot is generally indicative of a single class of fluorophores, all equally accessible to the quencher [28].

2.8 Time-resolved fluorescence measurements

Fluorescence decay measurements were performed with a Chronos-ISS fluorometer, (ISS, Champaign, IL, USA) using the phase shift and demodulation technique. The excitation source (295 nm) was a Laser diode and the emission was collected through a 337 long-pass filter (Edmund Optics, USA). As lifetime reference was used the 2, 5-diphenyl-1, 3, 4-oxadiazole and intensity decays were analyzed in terms of the multi-exponential model:

$$I(t) = I_0 e^{-t/\tau} = \sum \alpha i \, e^{-t/\tau} \qquad \textbf{Equation 2;}$$

where I_0 is the intensities at t = 0, τ is the lifetime of the fluorophore, α_i are the pre-exponential factors, and $\sum \alpha_i = 1.0$. For multi-component decays, the fractional intensity f_i of each decay time is given by

$$f_i = \alpha_i \tau_i / \sum \tau_i \, \alpha i \qquad \textbf{Equation 3;}$$

and the mean lifetime can be calculated as:

$$\tau = \sum f_i \, \tau_i \qquad \textbf{Equation 4 [28]}.$$

2.9 FT-IR measurements

Fourier transform infrared (FTIR) characterizations were performed on GluB in 20mM of deuterated sodium phosphate buffer pH 8.0, with a protein concentration of 6mg/mL in the absence and in the presence of Glu or Asp at 5mM concentration. FTIR spectra were collected and analyzed as previously described [29]. Briefly, 20µL of the sample solution was placed in a temperature-controlled transmission cell (Wilmad, Buena, NJ, U.S.A.) with two BaF_2 windows and a 100µm Teflon spacer. Absorption spectra were collected using the Varian 670-IR (Varian, Mulgrave, Australia) spectrometer, equipped with a nitrogen-cooled mercury cadmium telluride detector, under the following conditions: $2cm^{-1}$ spectral resolution, 25kHz scan speed, 500 scan co-addition, and triangular apodization. For the thermal denaturation experiments, sample solutions in the temperature-controlled cell were heated at 0.4°C/min from 25°C to 100°C, each spectrum being collected every ~1.74°C. The protein FTIR absorption spectra were obtained after subtraction of the appropriate reference spectra strictly collected under the same conditions. When necessary, the subtraction of residual vapour absorption was also performed [29, 30]. Second derivative spectra were obtained following the Savitsky-Golay method [31]. The Resolutions-Pro (Varian, Mulgrave, Australia) software was employed for spectra collection and analyses.

2.10 Statistical analysis

All measurements were been collect in triplicate and were been calculated the mean value and standard deviation. All fluorescence data were been normalized by the maximum and smoothed by Savitzky-Golay algorithm applied as a point of window 5 and as polynomial order 2.

3 Results and Discussion

3.1 Cloning, expression, and purification of GluB

GluB is a monomeric protein of 34kDa, involved in the uptake of the Glu inside cell. Recently, its three-dimensional structure was resolved at 1.9Å from the group of the Prof. Wang [23]. As a member of SBPs family, the GluB structure contains two similarly folded domains connected by a two or three-stranded β-sheet hinge, a characteristic folding structure feature of this class of protein (Fig. 1). The *gluB* gene was isolated from *C. glutamicum* ATCC 13032 by PCR without the N-terminal signal sequence of 78 bps necessary for protein translocation into the periplasm and cloned into the expression vector pET22b(+). The resulting plasmid pET22b(+)-*gluB*, conferring a C-terminal His_6-tag to GluB for affinity chromatography, was transformed into *E. coli* BL21(DE3) for heterologous gene expression. After cultivation of *E. coli* BL21 (DE3) pET22b(+)-*gluB* and expression of *gluB*, the resulting GluB protein was purified by two steps of purification (an affinity chromatography followed by a gel filtration chromatography). Starting from 4g of the humid pellet, 12mg of protein have been purified. The main steps of the purification procedure and the homogeneity of purified GluB are reported in Fig. 2A, 2B, 2C**.** The identity of GluB has been successfully verified by MALDI-TOF MS (data not shown).

3.2 CD results

CD experiments in Far-UV region were performed to investigate the temperature effect on GluB secondary structure. Fig. 3 shows GluB Far-UV spectra at 25°C in the absence and presence of 100μM Glu. The data shows that the Far-UV CD spectrum of GluB is characterized by the presence of two absorption bands: a positive band at 192nm related to the α-helix content and a negative band at 208 nm related to the β-sheet structure that change as consequence of the Glu binding. The thermal stability of the GluB in the absence and in the presence of Glu, in the range of temperatures 25-90°C, was studied. CD signal at 222nm was plotted as function of temperature and the data were

fitted with a single step transition curve. The obtained data show that the addition of Glu to the protein solution results in a marked increase of GluB melting temperature (T_m); then the T_m value increases from 40 to 53°C (Fig. 3 inset). These results suggest an increase of the stability of the secondary structure as a consequence of Glu binding. Similar effect was found for the binding of the Asp to GluB (data not shown).

3.3 Fluorescence results

The fluorescence steady state and fluorescence decay experiments were performed. In particular the effect of the binding Glu at GluB was estimated by a variation of its intrinsic tryptophan (W58 and W65) fluorescence emission [32]. The fluorescence emission spectrum (Fig. S1 of supplementary materials) of GluB in absence of Glu presents a fluorescence emission maximum peak centered at 333nm. This position is blue-shifted respect to the emission maximum of N-acetyl-tryptophanylamide (NATA) centred at 350nm (data not shown), suggesting that the tryptophanyl residues of GluB at 25°C are in buried and/or un-relaxed microenvironments. On contrary the fluorescence emission maximum of GluB/Glu complex reveals that the binding of 100μM Glu results in quenching of the protein fluorescence intensity about 30%. A fluorescence titration was performed in order to evaluate the affinity of GluB for Glu. The experiments were performed at 25°C and in Fig. 4A is reported the variation of fluorescence emission associated to the increase concentration of Glu in solution. The obtained variation of the fluorescence emission intensity at 333nm as function of the Glu concentration can be fit with a single binding isotherm model and we can determine, for Glu, an apparent $K_{d\ app}$ of 0.6nM at 25°C.

Also, we evaluated the effect of the temperature on the stability of GluB in the absence and in the presence of ligands. In Fig. 4B are reported the variations of maximum of the fluorescence intensity in function of the temperature (25-90°C) at pH 8.0. The result shows that as consequence of the binding of Glu the tertiary structure of GluB was stabilized and the T_m value of GluB increases from 40 °C to 50°C.

297 Since is well reported in literature that the binding capability of periplasmic glutamate binding
298 protein [20, 21] is often associate to the binding and transport of the Asp, as for the CD experiments
299 (Table 1), we have investigated the binding this amino acid to the GluB. In Fig. S2B of the
300 supplementary material is reported the variation of fluorescence intensity as consequence of
301 increase concentration of the Asp. Plotting the variation of fluorescence intensity with the increase
302 of Asp concentration, the apparent $K_{d\ app}$ values calculated result to be 0.014nM. Analogous
303 thermo-stability effect was obtained as consequence of ASP binding. The T_m value calculated for
304 the GluB/Asp complex was 55°C (Fig. S2B, Table 1).
305
306 ***3.4*** *Stern-Volmer quenching results*
307 With the aim to evaluate ligand binding-induced changes of Trp residue accessibility to the
308 quencher, we performed, in the absence and in the presence of Glu and Asp, acrylamide-quenching
309 experiments at 25°C. In Fig. 5 are reported the obtained results and Table 2 reports the values of the
310 Stern-Volmer quenching constant (K_{sv}) calculated for the GluB in the absence and in the presence
311 of Glu and Asp. At 25°C in the absence and in presence of the Glu, the Ksv values are 7,26 and
312 5,26 respectively. The data show a decrease of acrylamide quenching of Trp emission as
313 consequence of Glu addition. This result suggests that the Trp residues become less solvent
314 accessible following ligand bound. Similar effects have obtained with the Asp (Table 2). The linear
315 Stern-Volmer plot obtained data suggests that only one class of fluorophore is involved in the
316 quenching, as reported in Lakowicz [28].
317
318 *3.5 Lifetime measurements*
319 Finally, we have performed fluorescence decay experiments of GluB in the absence and in the
320 presence of Glu and Asp (Fig. 6). The data show that the best mathematical fit applicable with the
321 lifetime is a bi-exponential discrete distribution. The mean lifetime values reported in Table 3 do
322 not change in the absence and in the presence of the tested ligands [33].

3.6 FT-IR results

The secondary structures and thermal stability of GluB in the absence and in the presence of Glu or Asp were also investigated by FTIR spectroscopy. The second derivative spectra, whose minima correspond to absorption maxima, of GluB in the deuterated buffer are reported in Fig. 7A in the 1700-1500cm^{-1} spectral region, where the Amide I' band (1700-1600cm^{-1}) and the tyrosine side chain peak (around 1515cm^{-1}) can be observed. The Amide I' band is mainly due to the C=O peptide bond absorption whose peak position is sensitive to the protein's secondary structure [30, 34]. In order to resolve this band into its overlapping components, the second derivative analysis of the absorption spectra was performed [31]. The second derivative spectrum of GluB at 25°C displayed the main Amide I' component around 1638cm^{-1} that, along with the ~1694cm^{-1} peak, is assigned to the native β-sheets of the protein. The components at ~1656cm^{-1} and ~1675cm^{-1} are due to α-helical and turn structures, respectively. Finally, the peak at ~1615cm^{-1} can be assigned to amino acid side chains and/or to β-sheet structures in protein-protein interactions [30, 34]. Fig. 7A also shows second-derivative FTIR spectra of GluB as a function of temperature. No significant spectral changes were observed up to ~52°C. Above this temperature, the Amide I' components assigned to the protein native secondary structures (at ~1638, ~1656, ~1694, and ~1675cm^{-1}) decreased in intensity and disappeared. At 100°C, the GluB second derivative spectrum is dominated by a broad minimum at ~1646cm^{-1}, assigned to random coil structures [30, 34], indicating a thermal unfolding of the protein. The ~1615cm^{-1} peak slightly increased with the temperature at became more evident after cooling of the sample from 100°C to 25°C. These results indicated that a partial aggregation of the protein took place during the thermal treatments and that the thermal unfolding was irreversible, under our experimental conditions. Similar spectral behaviors were found in the thermal unfolding of GluB in the presence of 5mM of Glu (Fig. 7B), or Asp (data not shown).

In all cases, changes in the peak position of the IR tyrosine response around 1515cm^{-1} were observed also in the thermal treatments, as reported in Fig. 7C**.** These results indicated that Glu and

Asp induced a stabilization of GluB protein toward thermal unfolding. For a quantitative comparison, the intensity variation in the second derivatives of the native β-sheet component at ~1638cm^{-1} as a function of the temperature was employed for the Tm estimation (Fig. 7D, 7E). In the presence of Glu or Asp, the T_m value of GluB increased from ~68 to ~ 78°C (Fig. 7E). Therefore, these results indicated that the two amino acids increased the thermal stability of GluB both considering the protein secondary (Fig. 7D and 7C) structures.

4 Conclusion

Glu is the major excitatory neurotransmitter in the brain and it is used in food industry to enhance the food taste. Glu is routinely detected through analytical methods, with all the disadvantages (time-consuming, high cost etc.) associated with their application. So, the application of the biosensor technologies could be an alternative for the *on-field* Glu sensing. In this work we have performed a preliminary structural characterization of the GluB isolated from *C. glutamicum*. We explored the binding features and the effect of temperature on the protein stability in the absence and in the presence of Glu by CD, FT-IR and fluorescence techniques. The obtained results show a high affinity of Glu to GluB (Kd = 0,6nM) and the binding is associated with substrate-induced stability. Only in the FT-IR experiments, difference in the Tm values were registered resect the other two techniques and it is probably related to the different concentrations of the GluB used. Since in nature the transport of Glu into the cells is often associated also with the L-aspartate transport we have studied the binding of this aminoacid to GluB. Surprisingly, the results showed a high affinity of Asp respect the Glu and its binding is associated to a stabilizing effect on GluB structure.

Therefore, our experiments have shown that GluB have affinity for the Asp and this data suggest that GluB could be involved in both aminoacids uptake in the cell and GluB is a Glu/Asp binding protein (Glu/AspBP). In the future studies, we have plannned to investigate in details the binding discrimination between the two ligands (pH, ionic strength, etc.), but meantime we can conclude that GluB could be a good candidate as MRE to develop and optical reagentless biosensor for the detection of the Glu.

5 Acknowledgments

This project was partially funded by the CNR project NUTR-AGE (SD; MS; AC; AV).

6 References

[1] E. Palsson, J. Jakobsson, K. Sodersten, Y. Fujita, C. Sellgren, C.J. Ekman, H. Agren, K. Hashimoto, M. Landen, Markers of glutamate signaling in cerebrospinal fluid and serum from patients with bipolar disorder and healthy controls, Eur. Neuropsychopharmacol. 25(1) (2015) 133-40.

[2] D.C. Javitt, S.R. Zukin, Recent advances in the phencyclidine model of schizophrenia, Am. J. Psychiatry 148(10) (1991) 1301-8.

[3] D.M. Lovinger, G. White, F.F. Weight, Ethanol inhibits NMDA-activated ion current in hippocampal neurons, Science 243(4899) (1989) 1721-4.

[4] B.O. Rothbaum, Critical parameters for D-cycloserine enhancement of cognitive-behaviorial therapy for obsessive-compulsive disorder, Am. J. Psychiatry 165(3) (2008) 293-6.

[5] K. Niaz, E. Zaplatic, J. Spoor, Extensive use of monosodium glutamate: A threat to public health?, EXCLI journal 17 (2018) 273-278.

[6] O.V. Soldatkina, O.O. Soldatkin, B.O. Kasap, D.Y. Kucherenko, I.S. Kucherenko, B.A. Kurc, S.V. Dzyadevych, A Novel Amperometric Glutamate Biosensor Based on Glutamate Oxidase Adsorbed on Silicalite, Nanoscale research letters 12(1) (2017) 260.

[7] E. Swanepoel, M.M. de Villiers, J.L. du Preez, Fluorimetric method of analysis for d-norpseudoephedrine hydrochloride, glycine and l-glutamic acid by reversed-phase high-performance liquid chromatography, J. Chromatogr. A 729(1) (1996) 287-291.

[8] S. Tucci, C. Pinto, J. Goyo, P. Rada, L. Hernández, Measurement of Glutamine and Glutamate by Capillary Electrophoresis and Laser Induced Fluorescence Detection in Cerebrospinal Fluid of Meningitis Sick Children, Clin. Biochem. 31(3) (1998) 143-150.

[9] R.P. Berntsson, S.H. Smits, L. Schmitt, D.J. Slotboom, B. Poolman, A structural classification of substrate-binding proteins, FEBS Lett. 584(12) (2010) 2606-17.

405 [10] F.A. Quiocho, Atomic structures of periplasmic binding proteins and the high-affinity active
406 transport systems in bacteria, Philos. Trans. R. Soc. Lond. B Biol. Sci. 326(1236) (1990) 341-51;
407 discussion 351-2.
408 [11] M. Strianese, M. Staiano, G. Ruggiero, T. Labella, C. Pellecchia, S. D'Auria, Fluorescence-
409 based biosensors, Methods Mol. Biol. 875 (2012) 193-216.
410 [12] R.M. de Lorimier, J.J. Smith, M.A. Dwyer, L.L. Looger, K.M. Sali, C.D. Paavola, S.S. Rizk, S.
411 Sadigov, D.W. Conrad, L. Loew, H.W. Hellinga, Construction of a fluorescent biosensor family,
412 Protein Sci. 11(11) (2002) 2655-75.
413 [13] V. Scognamiglio, M. Staiano, M. Rossi, S. D'Auria, Protein-based biosensors for diabetic
414 patients, J Fluoresc 14(5) (2004) 491-8.
415 [14] M. Staiano, V. Scognamiglio, G. Mamone, M. Rossi, A. Parracino, M. Rossi, S. D'Auria,
416 Glutamine-binding protein from Escherichia coli specifically binds a wheat gliadin peptide. 2.
417 Resonance energy transfer studies suggest a new sensing approach for an easy detection of wheat
418 gliadin, J. Proteome Res. 5(9) (2006) 2083-6.
419 [15] W. Kronemeyer, N. Peekhaus, R. Kramer, H. Sahm, L. Eggeling, Structure of the gluABCD
420 cluster encoding the glutamate uptake system of Corynebacterium glutamicum, J. Bacteriol. 177(5)
421 (1995) 1152-8.
422 [16] L.E. Eggeling, M.E. Bott, Handbook of Corynebacterium glutamicum, Boca Raton: CRC Press
423 (2005).
424 [17] H. Yukawa, M. Inui, Corynebacterium glutamicum Biology and Biotechnology Microbiology
425 monographs, Springer, Heidelberg. (2013).
426 [18] V.F. Wendisch, J.M.P. Jorge, F. Perez-Garcia, E. Sgobba, Updates on industrial production of
427 amino acids using Corynebacterium glutamicum, World J. Microbiol. Biotechnol. 32(6) (2016) 105.
428 [19] S. Wieschalka, B. Blombach, M. Bott, B.J. Eikmanns, Bio-based production of organic acids
429 with Corynebacterium glutamicum, Microb. Biotechnol. 6(2) (2013) 87-102.

[20] S.A. Heider, V.F. Wendisch, Engineering microbial cell factories: Metabolic engineering of Corynebacterium glutamicum with a focus on non-natural products, Biotechnol. J. 10(8) (2015) 1170-84.

[21] M. Vogt, C. Brusseler, J.V. Ooyen, M. Bott, J. Marienhagen, Production of 2-methyl-1-butanol and 3-methyl-1-butanol in engineered Corynebacterium glutamicum, Metabolic engineering 38 (2016) 436-445.

[22] N. Kallscheuer, M. Vogt, A. Stenzel, J. Gatgens, M. Bott, J. Marienhagen, Construction of a Corynebacterium glutamicum platform strain for the production of stilbenes and (2S)-flavanones, Metabolic engineering 38 (2016) 47-55.

[23] Q. Liu, D. Li, Y. Hu, D.C. Wang, Expression, crystallization and preliminary crystallographic study of GluB from Corynebacterium glutamicum, Acta crystallographica. Section F, Structural biology and crystallization communications 69(Pt 6) (2013) 657-659.

[24] J. Sambrook, D. Russell, Molecular Cloning, Cold Spring Harbor Laboratory Press, Cold Spring Harbor, NY. vol. 1–3. (2001).

[25] H. Edelhoch, Spectroscopic determination of tryptophan and tyrosine in proteins, Biochemistry 6(7) (1967) 1948-54.

[26] J. Marienhagen, N. Kennerknecht, H. Sahm, L. Eggeling, Functional analysis of all aminotransferase proteins inferred from the genome sequence of Corynebacterium glutamicum, J. Bacteriol. 187(22) (2005) 7639-46.

[27] M.M. Moghaddam, M. Pirouzi, M.R. Saberi, J. Chamani, Comparison of the binding behavior of FCCP with HSA and HTF as determined by spectroscopic and molecular modeling techniques, Luminescence 29(4) (2014) 314-31.

[28] J.R. Lakowicz, Principles of Fluorescence Spectroscopy, Springer, New York, (3rd edition) (2006).

[29] D. Ami, S. Ricagno, M. Bolognesi, V. Bellotti, S.M. Doglia, A. Natalello, Structure, stability, and aggregation of beta-2 microglobulin mutants: insights from a Fourier transform infrared study in solution and in the crystalline state, Biophys. J. 102(7) (2012) 1676-84.

[30] A. Natalello, S.M. Doglia, Insoluble protein assemblies characterized by fourier transform infrared spectroscopy, Methods Mol. Biol. 1258 (2015) 347-69.

[31] H. Susi, D.M. Byler, Resolution-enhanced Fourier transform infrared spectroscopy of enzymes, Methods Enzymol 130 (1986) 290-311.

[32] N. Akbay, J.R. Lakowicz, K. Ray, Distance-dependent intrinsic fluorescence of proteins on aluminum nanostructures, Proc SPIE Int Soc Opt Eng 8234 (2012) 823417.

[33] P. Herman, M. Staiano, A. Marabotti, A. Varriale, A. Scire, F. Tanfani, J. Vecer, M. Rossi, S. D'Auria, D-trehalose/D-maltose-binding protein from the hyperthermophilic archaeon Thermococcus litoralis: the binding of trehalose and maltose results in different protein conformational states, Proteins 63(4) (2006) 754-67.

[34] A. Barth, Infrared spectroscopy of proteins, Biochim. Biophys. Acta 1767(9) (2007) 1073-101.

Table 1. Melting temperature of GluB in the absence and in the presence of Glu and Asp.

	Circular Dichroism Tm (°C)	**Steady-state Fluorescence Tm (°C)**
GluB	40 ± (0.8)	40 ± (0.8)
GluB + 100µM Glu	53 ± (0.3)	50 ± (0.4)
GluB + 100µM Asp	53 ± (1.2)	55 ± (1.4)

474 **Table 2.** Stern-Volmer analysis.

475

	K_d	R-Square
GluB	7.04±0.23	0.99652
GluB + 100μM Glu	5.26±0.13	0.99837
GluB + 100μM Asp	5.26±0.12	0.99853

476

477

Table 3. Lifetime analysis.

	Average Lifetime [ns]	χ^2
GluB	3.40	2.40
GluB + 100µM Glu	3.40	2.14
GluB + 100µM Asp	3.37	1.78

Figures

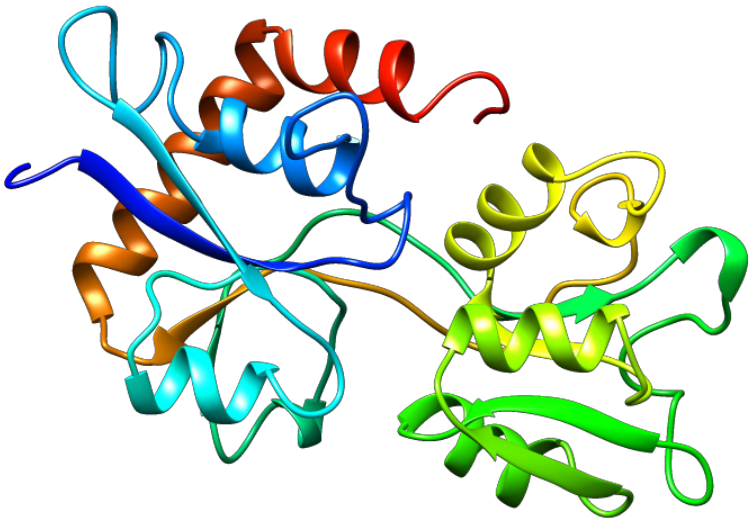

Figure 1. GluB homology model structure. The picture shows the GluB homology model calculated by Swiss-Model software and collected in Swiss-Model repository database (https://swissmodel.expasy.org/repository/uniprot//P48242).

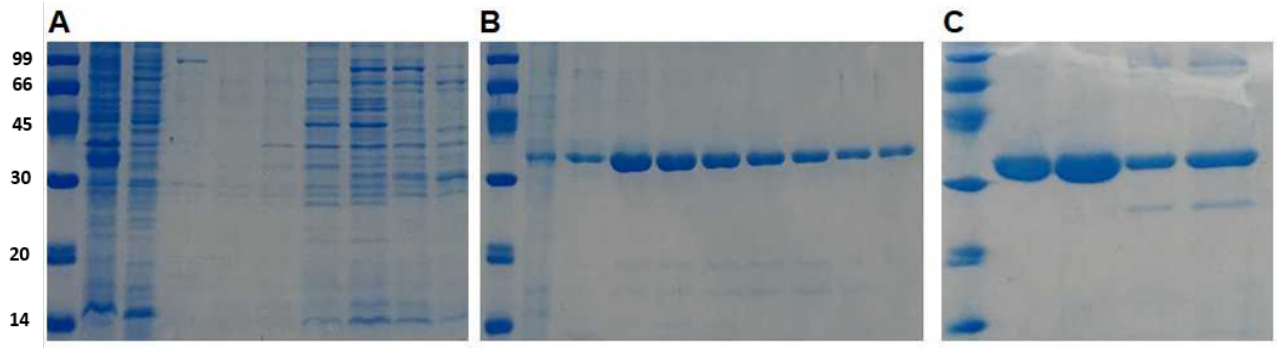

Figure 2. SDS-PAGE of the fractions obtained from chromatographic purification. (A) Affinity chromatography: (molecular weight standard, input, flow-through, wash, fractions 1 to 5 eluted at 50mM imidazole). **(B)** Affinity chromatography: (molecular weight standard, fractions 10, 11, 15, 20, 25, 30, 35, 40, 45 eluted at 50mM imidazole). **(C)** Size exclusion chromatography

(molecular weight standard, collected protein fractions after (line 2 and 3) and before (line 4 and 5) the gel filtration step).

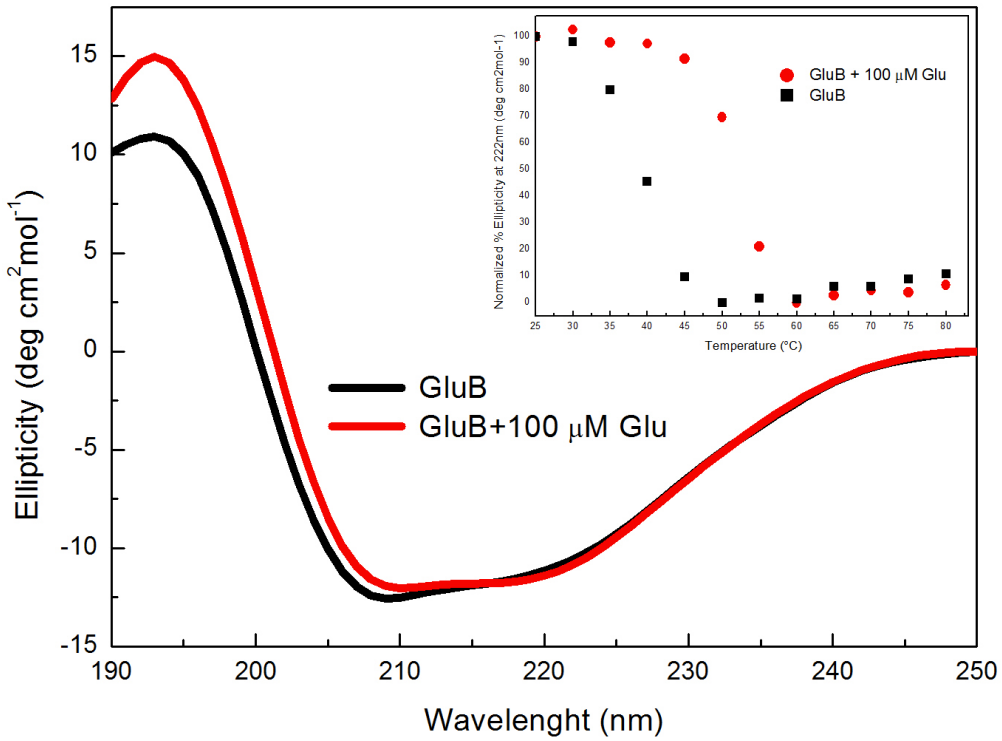

Figure 3. Circular dichroism results. Far-UV CD spectra of GluB in the absence and in presence of 100µM of Glu at 25°C. Inset: variation of the molar ellipticity at 222nm in the function of temperature in the absence and in the presence of Glu.

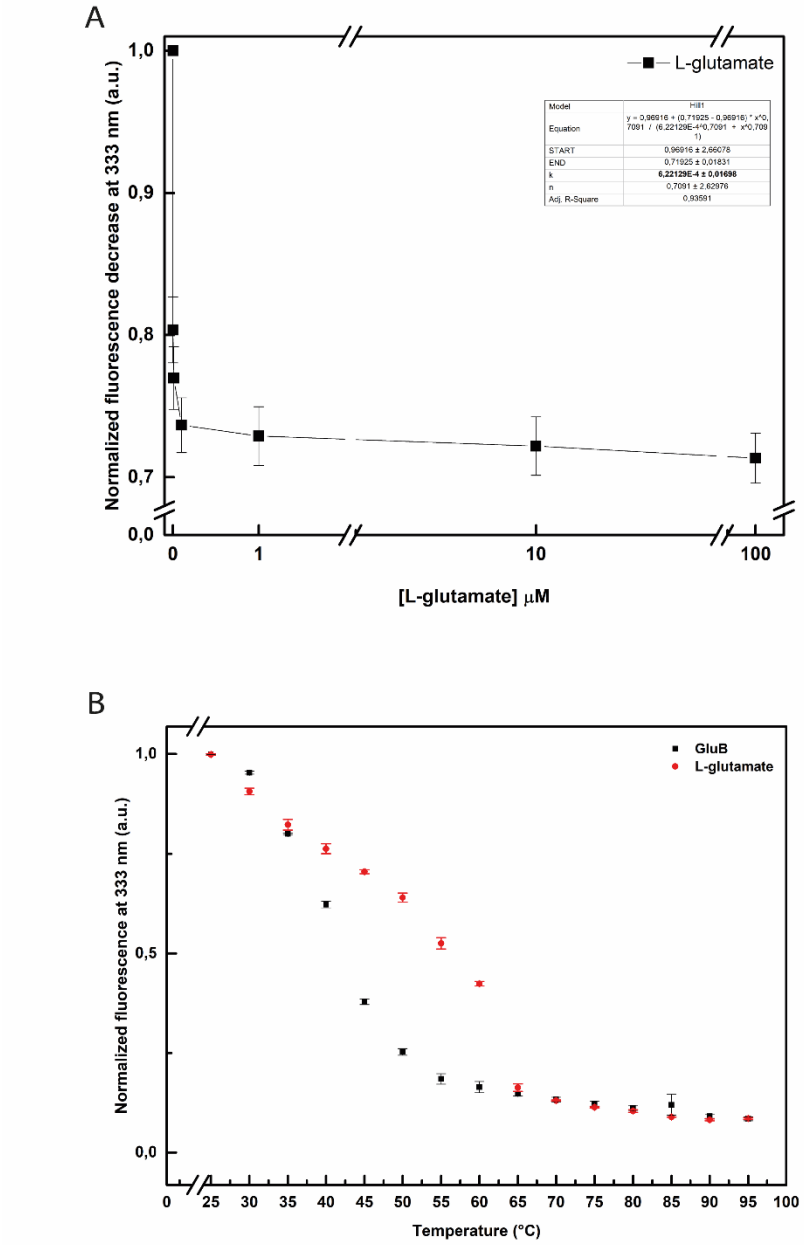

Figure 4. Fluorescence steady-state measurements: ligand binding and thermal stability evaluation. **(A)** Variation of the GluB fluorescence emission at 333nm in the presence of increase concentration of Glu. Excitation of two Trp residues (W58 and W65) was performed at 295 nm in 5mM phosphate buffer, pH 8.0. **(B)** GluB thermal unfolding: variation of the Trp emission in the absence and in presence of 100µM Glu. Fluorescence measurements obtained at an excitation wavelength of 295 nm in 5 mM phosphate buffer at pH 8.0.

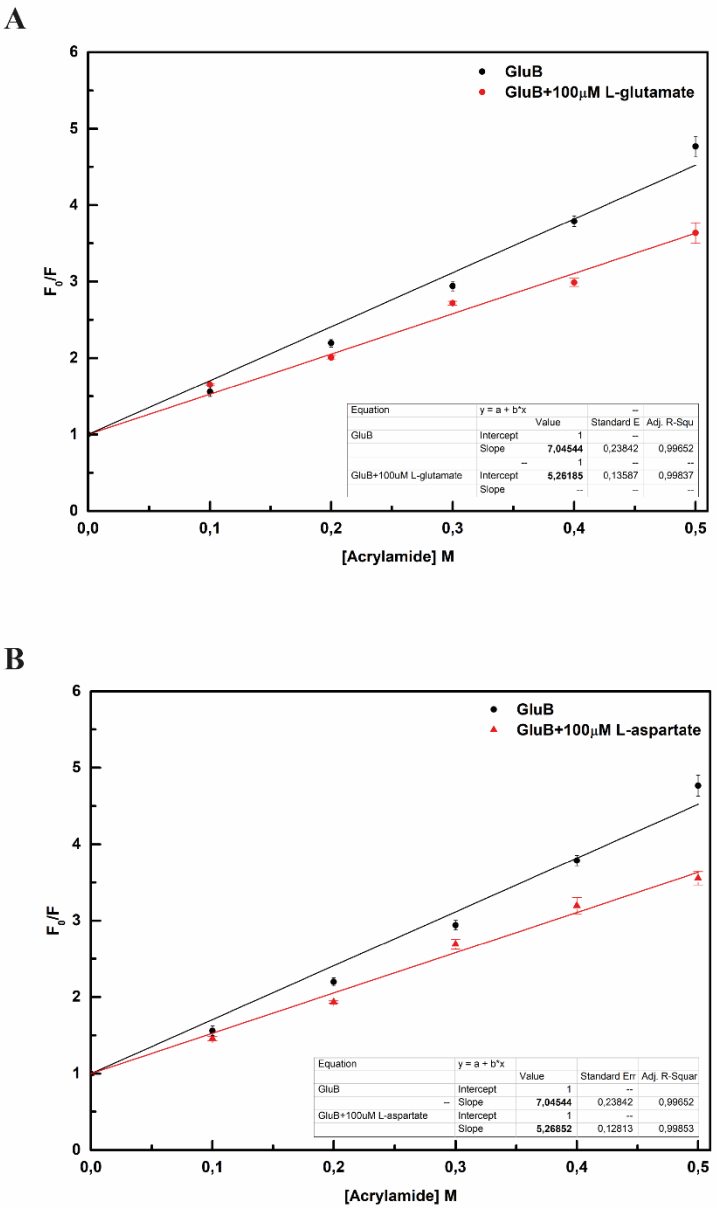

508

509 **Figure 5. Quenching measurements.** Steady-state acrylamide quenching of GluB in the absence

510 (closed circles) and in the presence (red circles) of 100μM Glu, and in the presence of 100μM Asp

511 (red triangles). The measurements performed at 25°C.

512

A

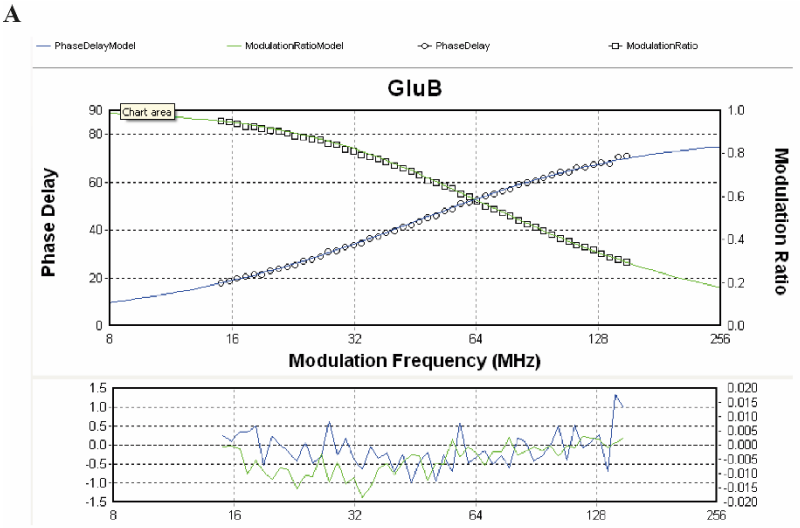
PhaseDelayModel
ModulationRatioModel
PhaseDelay
ModulationRatio
GluB
Chart area
Phase Delay
Modulation Ratio
Modulation Frequency (MHz)

B

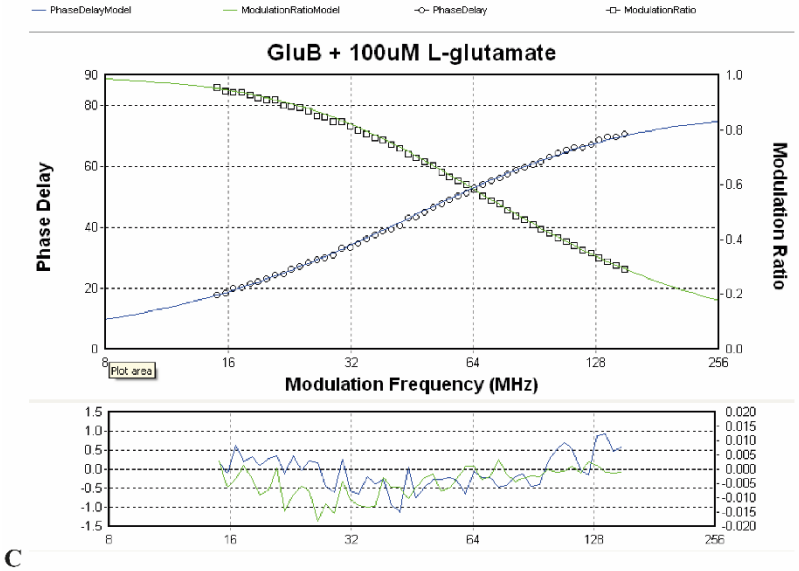
PhaseDelayModel
ModulationRatioModel
PhaseDelay
ModulationRatio
GluB + 100uM L-glutamate
Plot area
Phase Delay
Modulation Ratio
Modulation Frequency (MHz)

C

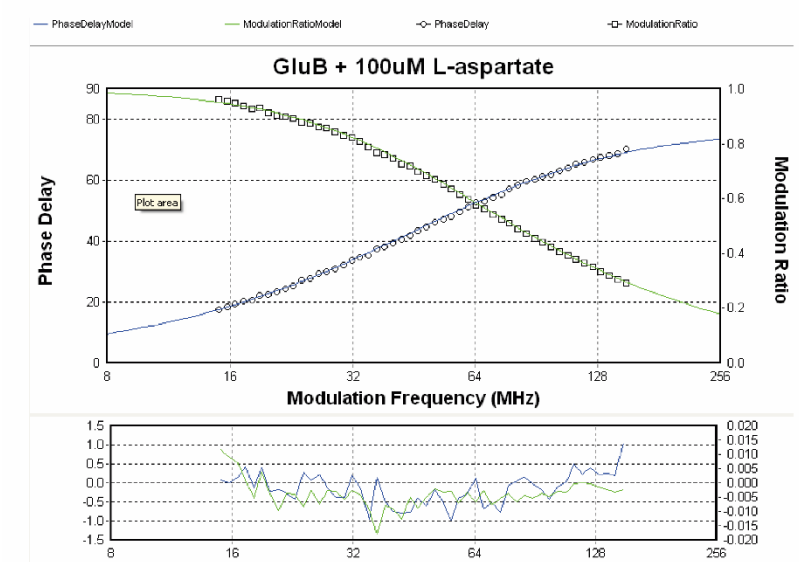
PhaseDelayModel
ModulationRatioModel
PhaseDelay
ModulationRatio
GluB + 100uM L-aspartate
Plot area
Phase Delay
Modulation Ratio
Modulation Frequency (MHz)

513

Figure 6. Lifetime measurements. In the figures are reported the bi-exponential fitting analysis for **(A)** GluB, **(B)** GluB/Glu, and **(C)** GluB/Asp. The bottom part of each panel reports the residual analysis of the fitting procedure.

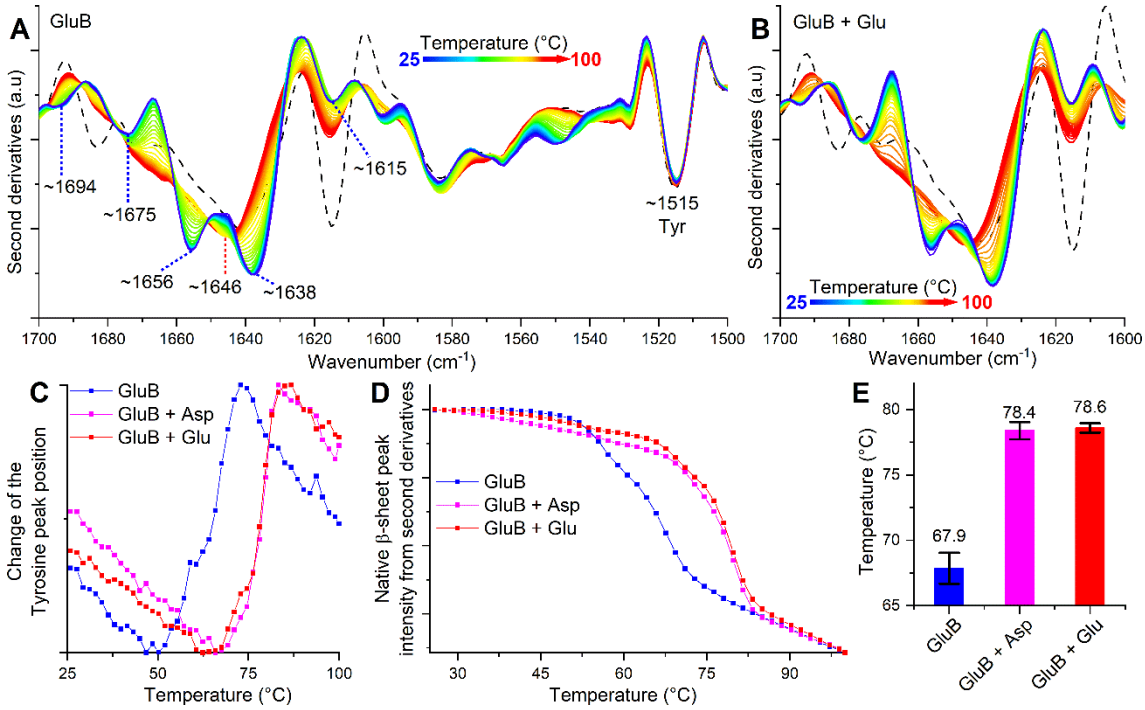

Figure 7. GluB thermal unfolding monitored by FTIR. (A) Second derivative FTIR spectra of 6 mg/mL GluB in deuterated phosphate buffer at different temperatures between 25 and 100°C. The spectrum taken at 25°C after the thermal treatment (dashed line) is also reported. Spectra are shown in the 1700-1500cm^{-1} regions. The peak position of the main components is indicated. **(B)** Second derivative FTIR spectra of 6 mg/mL GluB and 5mM Glu in deuterated phosphate buffer at different temperatures between 25 and 100°C. The spectrum taken at 25°C after the thermal treatment (dashed line) is also reported. Spectra are shown in the 1700-1600 cm^{-1} region. **(C)** The temperature dependence of the peak position of the ~1515 cm^{-1} tyrosine band, taken from second derivative spectra, is reported for GluB in the absence and in the presence of 5mM of Glu or Asp. **(D)** The temperature dependence of the native β-sheet peak intensity at ~1638cm^{-1}, taken from second derivative spectra, is reported for GluB in the absence and in the presence of 5mM of Glu or Asp.

(E) Tm values obtained from the data of panel **(D)**. Error bars are the standard deviations of independent thermal unfolding experiments.

7 Supplementary materials

Fig. S1. Steady state fluorescence measurements: **(A)** normalized fluorescence emission spectra of the L-glutamate titration experiments, and **(B)** normalized fluorescence emission spectra of the L-aspartate titration experiments.

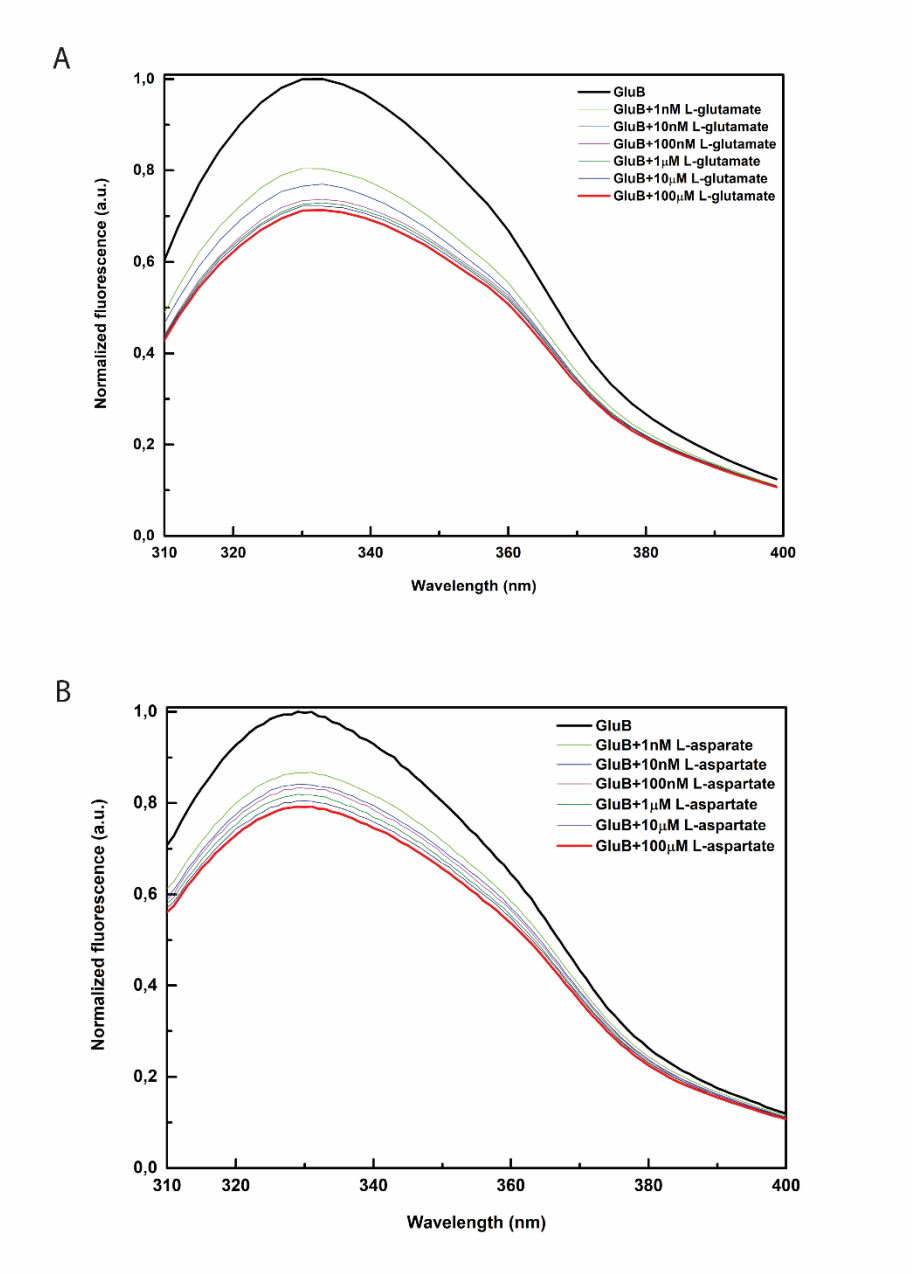

Fig. S2. Steady state fluorescence measurements: **(A)** GluB/Asp binding curve and **(B)** GluB/Asp thermal stability.